

See discussions, stats, and author profiles for this publication at: <https://www.researchgate.net/publication/231679860>

# Self-Assembly of Perfluorodecanoic Acid with Cationic Copolymers: Ultra-Low Energy Surfaces and Mesomorphous Structures

ARTICLE *in* LANGMUIR · JULY 1998

Impact Factor: 4.46 · DOI: 10.1021/la971379e

---

CITATIONS

35

---

READS

31

2 AUTHORS, INCLUDING:



**Andreas F Thünemann**

Bundesanstalt für Materialforschung und -pr...

178 PUBLICATIONS 4,961 CITATIONS

SEE PROFILE

# Self-Assembly of Perfluorodecanoic Acid with Cationic Copolymers: Ultra-Low Energy Surfaces and Mesomorphous Structures

Andreas F. Thünemann and Kai Helmut Lochhaas

Max-Planck Institut für Kolloid- & Grenzflächenforschung, Kantstrasse 55,  
D-14513 Teltow-Seehof, Germany

Received December 16, 1997. In Final Form: May 29, 1998

Solid complexes of poly[diallyldimethylammonium chloride)-*co*-(*N*-methyl-*N*-vinylacetamide)] with perfluorodecanoate were prepared with a 1:1 stoichiometry. The surface energies of the fluorinated complexes were in the range of 13 to 15 mN/m independent of the fluorine amount present. This result was attributed to the formation of a surface of closely packed trifluoromethyl groups. All of the complexes form thermally stable, self-organized mesophases with body-centered cubic or body-centered tetragonal symmetry. The unit cell volume shrinks from 100 to 40 nm<sup>3</sup> with increasing charge density of the polyelectrolyte. This shrinkage is accompanied by an increase in the bulk density from 1.44 to 1.87 g/cm<sup>3</sup>. From wide-angle X-ray scattering it was derived that the packing order of the perfluoroalkyl chains strongly depends on the charge density and increases in a stepwise manner from amorphous to crystalline.

## 1. Introduction

The systematic preparation of low-energy surfaces performed via self-assembly of polyelectrolyte–surfactant complexes (PE–surfs) is of fundamental interest in supramolecular science as well as of high technological impact. Especially for coatings there seems to be a great variety of applications for these new materials. Because of their easy preparation, such coatings are very promising, (e.g., as self-cleaning surfaces or as very thin protective coatings for walls that are prone to contamination, like graffiti). The growing field of solid PE–surfs<sup>1–5</sup> has been reviewed recently.<sup>4,6</sup> Many of these complexes show a pronounced tendency to form well-ordered liquid crystalline-like structures with high mechanical and thermal stability. In the field of fluorinated PE–surfs, little is known and, up to now, only systems with lamellar mesophase structures and one example of a two-dimensional (2D) hexagonal mesophase have been found.<sup>7,8</sup> In this article we report on pseudo-cubic and tetragonal mesophases, formed by complexation of perfluorodecanoic acid **2** with cationic copolymers of diallyldimethylammonium chloride and *N*-methyl-*N*-vinylacetamide **1**, resulting in poly(diallyldimethylammonium)-*co*-(*N*-methyl-*N*-vinylacetamide) perfluorodecanonate **3**. The complexation is shown schematically in Figure 1. To investigate the influence of the charge density on the structure, five polymer complexes were prepared, varying in the amount of diallyldimethylammonium units (i.e., 25, 47, 65, 83, and 100 mol%). Recently, copolymer **1** was used to study

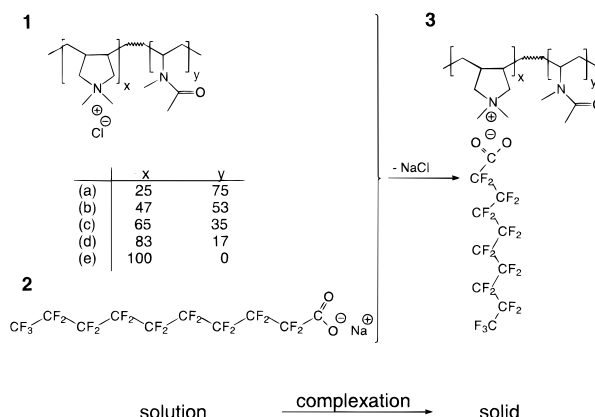


**Figure 1.** Sketch of complex formation: **(1)** poly[diallyldimethylammonium chloride)-*co*-(*N*-methyl-*N*-vinylacetamide)]; **(2)** perfluorodecanoic acid; **(3)** stoichiometric polyelectrolyte surfactant complex.

the influence of cationic polyelectrolytes on structure formation in lamellar liquid crystalline systems in aqueous solution.<sup>9</sup> It was found that the lamellar liquid-crystals of a sodium dodecyl sulfate/decanol/water mixture remained stable up to at least a polymer content of 10% (w/w). In contrast, we investigate an undiluted, salt-free binary system with 1:1 stoichiometry with respect to the charges. This represents, similar to diblock copolymers, the simplest case for studying the various aspects of microphase transition.

## 2. Experimental Section

**A. Materials.** The surfactant perfluorodecanoic acid (98%, Aldrich) was used as received. The copolymers poly[diallyldimethylammonium chloride)-*co*-(*N*-methyl-*N*-vinylacetamide)] were synthesized by radical polymerization with the initiator 2,2'-azobis(2-amidinopropane dihydrochloride) (V50, Wako) in water at 50 °C. The experimental conditions are described elsewhere.<sup>9</sup> All polymers were purified by ultrafiltration (membrane 10 K) and subsequently freeze-dried. The composition of the polymers

- (1) Ponomarenko, E. A.; Waddon, A. J.; Tirrell, D. A.; MacKnight, W. J. *Langmuir* **1996**, *12*, 2169–2172.
- (2) Ponomarenko, A.; Waddon, A. J.; Bakeev, K. N.; Tirrell, D. A.; MacKnight, W. J. *Macromolecules* **1996**, *29*, 4340–4345.
- (3) Antonietti, M.; Conrad, J.; Thünemann, A. *Macromolecules* **1994**, *27*, 6007–6011.
- (4) Antonietti, M.; Burger, C.; Thünemann, A. *Trends in Polymer Sci.* **1997**, *8*, 262–267.
- (5) Antonietti, M.; Wenzel, A.; Thünemann, A. *Langmuir* **1996**, *12*, 2111–2114.
- (6) Ober, C. K.; Wegner, G. *Adv. Mater.* **1997**, *9*, 17–31.
- (7) Antonietti, M.; Henke, S.; Thünemann, A. *Adv. Mater.* **1996**, *8*, 41–45.
- (8) Lochhaas, K. H.; Thünemann, A.; Antonietti, M. *Fluorine in Coatings II*; Paint Research Association: Teddington, UK, 1997.

- (9) Ruppelt, D.; Kötz, J.; Jaeger, W.; Friberg, S. E.; Mackay, R. A. *Langmuir* **1997**, *13*, 3316–3319.

was analyzed by chloride titration and  $^{13}\text{C}$  NMR spectroscopy. The stoichiometry of diallyldimethylammonium chloride to *N*-methyl-*N*-vinylacetamide was (a) 25:75, (b) 47:53, (c) 65:35, (d) 83:17, or (e) 100:0 (see Figure 1). The weight- and number-average molecular weights ( $M_w$  and  $M_n$ , respectively) of the compounds were determined by gel permeation chromatography (GPC, 0.5 mol/dm<sup>3</sup> NaNO<sub>3</sub>, Progel-TSK-PW column by Tosohaas, refraction index and light scattering detector). The molecular weights for the compounds in Figure 1 are (a)  $M_w = 177\,000$  g/mol,  $M_n = 128\,000$  g/mol, (b)  $M_w = 162\,000$  g/mol,  $M_n = 113\,000$  g/mol, (c)  $M_w = 205\,000$  g/mol,  $M_n = 151\,000$  g/mol, (d)  $M_w = 238\,000$  g/mol,  $M_n = 163\,000$  g/mol, and (e)  $M_w = 623\,000$  g/mol,  $M_n = 187\,000$  g/mol.

**B. Preparation.** A 1:1 equivalent (equiv) of perfluorodecanoic acid (0.5 g) was soluted in 50 mL of distilled water, and the pH was adjusted to 9 with 10% (w/w) NaOH. At 60 °C, the solution was stirred and a solution of 1.0 equiv of polyelectrolyte in 50 mL of water was added in a dropwise manner. The stoichiometry was calculated with respect to the charges. After adjusting the pH to 3 with 10% HCl, a solid complex was obtained as a white precipitate. The complex was separated, washed three times with 20 mL of 60 °C hot water, and dried for 12 h at 0.1 mbar. Elemental analysis for the complexes delivered [observed (calculated for a 1:1 stoichiometry)] **3a**: C, 37.1 (42.3); H, 4.1 (4.6); N, 4.7 (6.0); **3b**: C, 34.8 (37.8); H, 3.3 (3.5); N, 3.2 (4.0); **3c**: C, 31.3 (35.9); H, 2.5 (3.0); N, 2.4 (3.1); **3d**: C, 30.1 (34.6); H, 2.4 (2.7); N, 2.2 (2.6); **3e**: C, 30.9 (33.8); H, 2.7 (2.5); N, 2.2 (2.2).

**C. Methods.** Wide-angle X-ray scattering (WAXS) measurements were carried out with a Nonius PDS120 powder diffractometer in transmission geometry. A FR590 generator was used as the source for Cu K $\alpha$  radiation, and monochromatization of the primary beam was achieved with a curved Ge crystal. The scattered radiation was measured with a CPS120 position sensitive detector (Nonius, Germany). The resolution of this detector is better than 0.018°. Small angle X-ray scattering (SAXS) measurements were recorded with a X-ray vacuum camera with pinhole collimation (Anton Paar, Austria; model A-8054) equipped with image plates (type BAS III, Fuji, Japan). The image plates were read with a MACScience Dip-Scanner IPR-420 and IP reader DIPR-420 (Japan). Differential scanning calorimetry (DSC) measurements were performed on a Netzsch DSC 200 (Germany). The samples were examined at a scanning rate of 10 K/min by applying one cooling and two heating scans. First and second heating traces were essentially identical. Polarized light optical microscopic observations of the films were performed with a Zeiss DMRB microscope (Germany). Contact angles were determined by the sessile drop technique with optics from Carl Zeiss/Jena. Hexadecane was used as the test liquid. The droplet size was controlled with a Hamilton syringe. The contact angles were averaged over four measurements.

### 3. Results and Discussion

**A. Contact Angle Measurements.** Films for contact angle measurements were prepared by spraying 1% (w/w) complex solutions on different substrates; e.g., silicon wafers, glass panes, polished aluminium plates, and painted aluminium sheets. The latter were painted with a fast-drying automobile acrylic paint. The films were dried at 20 °C for 1 day and, for further removal of traces of solvent, the coated substrates were placed under reduced pressure at  $10^{-1}$ – $10^{-2}$  mbar and 30 °C for 12 h. This procedure results in optically transparent films with thicknesses of 5 to 30  $\mu\text{m}$ , smooth appearances, and good mechanical adhesion between the substrate and complex film. The film thicknesses were estimated from the weight increase of the wafers after coating. Table 1 lists the advancing and receding angles of hexadecane placed on films of the various complexes. From these values surface energies in the range of 13 to 15 mN/m can be estimated by averaging advancing and receding angles. It should be stressed that these values are valid for hexadecane as a test liquid and are not extrapolated, e.g., from a Zisman

**Table 1. Contact Angles of Hexadecane on Films of Complexes 3a to 3e and Their Glass Transition Temperatures  $T_g$**

complex	fluorine content % (w/w)	contact angle (deg)		$T_g$ , °C
		advancing	receding	
<b>a</b>	38.6	79 $\pm$ 3	58 $\pm$ 3	74 $\pm$ 5
<b>b</b>	48.1	72 $\pm$ 4	60 $\pm$ 4	70 $\pm$ 5
<b>c</b>	52.1	77 $\pm$ 3	53 $\pm$ 6	60 $\pm$ 5
<b>d</b>	54.8	71 $\pm$ 5	62 $\pm$ 2	50 $\pm$ 5
<b>e</b>	56.5	76 $\pm$ 4	62 $\pm$ 3	30 $\pm$ 10

plot<sup>10</sup> that usually results in significantly lower critical surface tensions. All films show hysteresis in the range 9–24°. This range is comparable to, or lower than, that of polytetrafluoroethylene (~25°),<sup>11</sup> fluorinated poly( $\alpha$ ,L-glutamate)s (20–30°),<sup>12</sup> and fluorinated low-surface energy polystyrene (14–42°).<sup>13</sup> In general, differences between advancing and receding contact angles can be a result of surface heterogeneity, roughness, rearrangement, and deformability.<sup>14</sup> Table 1 shows that neither the advancing nor the receding contact angles depend on the total fluorine content. Zisman<sup>10</sup> demonstrated that the surface energy depends on both the constitution and structure of the surface and that the lowest surface energy is that of closely packed trifluoromethyl groups.<sup>10</sup> The contact angles for the complexes **3a**–**3e** indicate a highly ordered fluorocarbon surface. For fluorinated side-chain polymers, this is found only when a significant degree of side-chain crystallization is observed.<sup>12,13</sup> In the case of the complexes **3a**–**3e** the situation is quite different: WAXS measurements show that the molecular ordering of the fluoralkyl chains vary from amorphous (**3a**, **3b**, **3c**) over laterally ordered (**3d**) to crystalline (**3e**), but this does not affect the contact angle. Therefore, it can be concluded that the surface structure of the complex films is enriched strongly with CF<sub>3</sub> groups, independent of crystallinity.

**B. Thermal Analysis.** The phase behavior of the complexes was investigated DSC. For all the complexes, broad glass transitions were found when the temperature decreased with increasing fluorine content [from 74 (**3a**) to 30 °C (**3e**), see Table 1]. For the complexes **3a** to **3d**, no melting peaks could be observed at temperatures lower than 150 °C. At higher temperatures, the polymers decompose, which is the limiting factor of the complex stability. Complex **3e** shows a melting peak at 46 °C. The melting point of perfluorodecanoic acid is 83–85 °C and, therefore, a melting of free acid can be excluded. We attribute the peak of complex **3e** to a side-chain crystallization similar to that observed for perfluorooctyl-substituted polystyrene<sup>13</sup> and fluorinated polyglutamates.<sup>12</sup> The decrease of the glass transition temperature ( $T_g$ ) from **3a** to **3e** is somewhat surprising because the amount of ionic moieties increases in the same order, and for this reason one may expect an increasing  $T_g$ . On the other hand, it is known for nonionic copolymers that  $T_g$  can be reduced by increasing the fraction of fluorinated monomers. For example, copolymers of styrene and perfluorooctyl-substituted styrene show a strong decrease in  $T_g$  with increasing perfluorooctyl content.<sup>13</sup> Obviously, in the case of the complexes **3a** to **3e**, the effect of an

(10) Zisman, W. A. *Contact Angle, Wettability, and Adhesion*; Advances in Chemistry Series 43; American Chemical Society: Washington, DC, 1964.

(11) Sperati, C. A. *Physical Constants of Fluoropolymers*, 3 ed.; John Wiley: New York, 1996.

(12) Dessipri, E.; Tirrell, D. A.; Atkins, E. D. T. *Macromolecules* **1996**, *29*, 3545–3551.

(13) Höpken, J.; Möller, M. *Macromolecules* **1992**, *25*, 1461–1467.

(14) de Gennes, P. G. *Rev. Mod. Phys.* **1985**, *57*, 827–863.

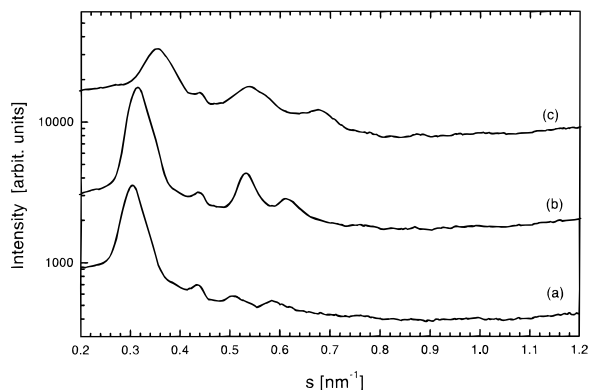


**Figure 2.** Small-angle X-ray diagrams of complexes **3a** to **3c**.

**Table 2.** X-ray Diffraction Data for the Body-Centered Pseudocubic Complexes **3a** to **3c** and the Body-Centered Tetragonal Lattice of Complexes **d** and **e** ( $s$  is the Scattering Vector Defined as  $s = 2/\lambda \sin(\theta)$ )

$hkl$	$s_{\text{obs}}, \text{nm}^{-1}$	$s_{\text{cal}}, \text{nm}^{-1}$	intensity obs
<b>Complex a</b>			
110	0.302	0.303	vs
200	0.44	0.429	w
211	0.503	0.526	w
220	0.585	0.607	w
222	0.762	0.743	vw
<b>Complex b</b>			
110	0.313	0.314	vs
200	0.434	0.444	w
211	0.530	0.544	s
200	0.612	0.629	w
222	0.761	0.769	vw
<b>Complex c</b>			
110	0.348	0.354	vs
200	0.538	0.500	s
220	0.690	0.707	w
222	0.883	0.866	vw
<b>Complex d</b>			
101	0.393	0.402	s
110	0.439	0.442	s
002	0.492	0.506	vs
200	0.590	0.625	w
112	0.678	0.672	vw
211	0.761	0.743	vw
220	0.873	0.884	w
301	0.983	0.971	vw
<b>Complex e</b>			
101	0.377	0.377	s
110	0.407	0.416	w
002	0.467	0.471	vs
211	0.700	0.698	w
220	0.850	0.832	vw
222	0.957	0.955	vw
312	1.050	1.042	w

increasing chain mobility, caused by a higher fluorine content, is predominant compared with the reduced mobility due to a higher amount of ionic species.

**C. Small-Angle X-ray Scattering.** SAXS experiments were used to identify the ordered-state symmetry of the complexes. The scattering diagrams of complex **3** films with the copolymer composition **a** to **c** are presented in Figure 2. Each pattern exhibits four strong reflections with relative positions of  $1:\sqrt{2}:\sqrt{3}:2$ . Obviously, these complexes are mesomorphously ordered. The SAXS data obtained are not of sufficient quality to unambiguously identify the space group. Nevertheless, the data prove the existence of a three-dimensional long-range ordered structure. From the positions of the reflections, a cubic mesophase can be assumed, either a primitive cubic ( $cP$ )

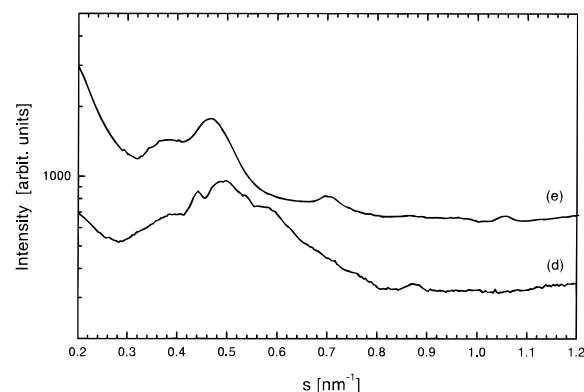


**Figure 3.** Small-angle X-ray diagrams of complexes **3d** and **3e**.

**Table 3.** Lattice Parameters and Density of Complexes **a** to **e**

complex	copolymer $x:y$ (mol %)	$a$ , nm	$c$ , nm	$V$ , $\text{nm}^3$	lattice type <sup>a</sup>	density, $\text{g}/\text{cm}^3$
<b>a</b>	25:75	4.66		101	$cI$	1.44
<b>b</b>	47:53	4.50		91	$cI$	1.52
<b>c</b>	65:35	4.00		64	$cI$	1.72
<b>d</b>	83:17	3.20	3.95	40	$tI$	1.82
<b>e</b>	100:0	3.40	4.25	49	$tI$	1.87

<sup>a</sup>  $cI$  = body-centered cubic;  $tI$  = body-centered tetragonal.

or body-centered cubic ( $cI$ ). Unfortunately, the position of the 7th-order reflection needs to be observed to distinguish between both lattices. Tentatively, we assume the existence of  $cI$  lattices. The corresponding reflection positions and indexing are listed in Table 2. From the distribution of reflections we conclude that the complexes **3a** to **3c** are isomorphous but with a significantly different unit cell volume. As seen in Figure 2, the maximum positions from **a** to **c** shift towards higher values. Therefore, the unit cell volume is shrinking with a higher charge density of the polyelectrolyte from complex **3a** to **3c**. The lattice constants are  $a_a = 4.66$  nm,  $a_b = 4.50$  nm and  $a_c = 4.00$  nm.

The SAXS diagrams of the complexes **3d** and **3e** (see Figure 3) characteristically differ from the others. It is obviously clear that not the first, but the second (**3e**) and the third (**3d**) reflection are the most intense. This behavior and the reflection positions can be assigned to a body-centered tetragonal lattice (see Table 2). For complex **3d**, the lattice constants were determined to be  $a_d = 3.20$  nm and  $c_d = 3.95$  nm, and for complex **3e**, these constants are  $a_e = 3.40$  nm and  $c_e = 4.25$  nm. Both complexes show a distinctly lower cell volume than the cubic ones. The lattice parameters and cell volumes are summarized in Table 3.

In the last few years we found that the type of mesophase of PE-surfs can often be derived from that of the surfactant in concentrated solution. The PE-surfs of dialkyldimethylammonium surfactants or those of soy bean lipids exhibit variations of the lamellar morphology.<sup>3,15</sup> Therefore, for interpretation of the SAXS data it is useful to refer to the phase diagram of the surfactants. Cubic phases are quite common in amphiphilic lipid systems with hydrocarbon chains, but because of poor SAXS data quality, the determination of their space group is often a problem.<sup>16</sup> Usually the space groups are present in the phase diagram between the other main phases and,

(15) Antonietti, M.; Kaul, A.; Thüenemann, A. *Langmuir* **1995**, *11*, 2633–2638.

(16) Fontell, K. *Coll. Polymer. Sci.* **1990**, *268*, 264–285.



therefore, have been given the generic term "intermediate phases." In contrast to the phase diagrams of hydrocarbon-containing surfactants, the phase diagrams of perfluorosurfactants are generally much simpler. In many cases, both the cubic and the hexagonal phase do not exist and the lamellar phase borders on an isotropic micellar solution. In some cases, the lamellar phase begins right at the critical micelle concentration.<sup>17</sup> This result is probably due to the larger cross-section and the rigidity of the perfluorinated chain compared with an alkyl chain. The phase diagrams for the single-chain perfluorosurfactants have a large similarity to double-chain surfactants of the hydrocarbons, which preferably form lamellar mesophases. Furthermore, it is known that perfluorocarboxylates form disk-like micelles, and generally one finds disk-like micelles in the vicinity of a lamellar phase.<sup>17</sup>

To a limited extent, the complexes **3a** to **3e** can be considered concentrated perfluorocarboxylate solutions in which the solvent is substituted by a polymer. Consequently, lamellar mesophases for complexes **3a** to **3e** are expected. The intrinsic tendency of **2** to form a lamellar mesophase to minimize the interfacial area seemed to be in contrast with the cubic or tetragonal lattice found by SAXS. But, in contrast to a concentrated aqueous solution of a perfluorinated acid, the mobility of the acid moieties in the complexes is strongly restricted because of anchoring of the carboxylic head groups to cationic diallyldimethylammonium moieties. In other words, the cationic and anionic groups are strongly coupled in their movement and in their spatial pattern. It is known from hydrocarbon-containing complexes that complexation may result in frustrated interfaces that lead to interesting structural variations of the lamellar surfaces.<sup>3,5,15</sup> Moreover, in a series of PE-surfs of copolymers of acrylic acid and *N*-alkylacrylamides, Antonietti and Maskos<sup>18</sup> found lamellar mesophases showing periodic undulations of hexagonal and disordered cubic symmetry.

Similarly, it has been reported for concentrated solutions of perfluorocarboxylates that deviations from the simple lamellar symmetry exist. For example, in the hexagonal/lamellar transition region of lithium perfluorooctanoate in water, Tiddy et al.<sup>19</sup> found an intermediate structure of tetragonal symmetry. That phase has a repeated layer ordering that is closely related to the lamellar structure. On the basis of X-ray and NMR diffusion measurements, Tiddy claims the surfactant layers consist of a tetragonal array of rods joined in groups of four, further ordered in three dimensions in a body-centered lattice. Thus, the intermediate phase for that perfluorooctanoate is a lamellar structure where the layers contain a regular array of holes through which water and ions can rapidly diffuse.

For an interpretation of the cubic pattern of complexes **3a** to **3c** and that of the tetragonal complexes **3d** and **3e** we propose a perforated lamellar structure as a possible unique building block. The lamellae are arranged in a well-defined *abab...* stacking pattern of perforated layers with a clear quadratic periodicity in plane direction. A model of the structure is shown in Figure 4. The lamellar distance is the half of the lattice constant perpendicular to the lamellae ( $l_a = a_d/2 = 2.33$  nm,  $l_b = a_b/2 = 2.25$  nm,  $l_c = a_d/2 = 2.00$  nm,  $l_d = c_d/2 = 1.98$  nm,  $l_e = c_d/2 = 2.13$  nm). The distance of the perforations within the lamellar

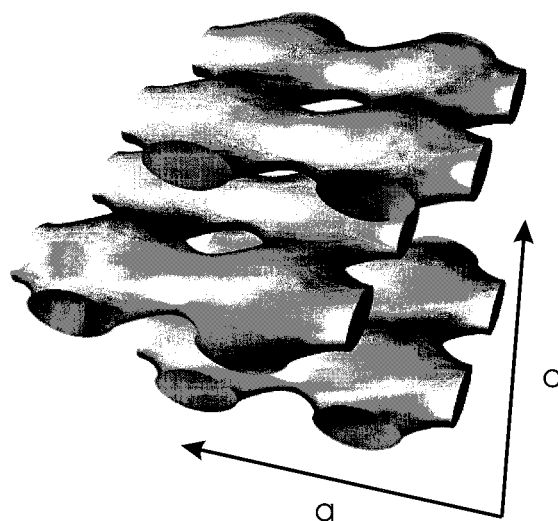


**Figure 4.** Model of the perforated layer structure. Within this structure, the polyelectrolyte phase is plotted grey. The surfactant molecules fill the interlayer space.

plane is identical to the lattice constants in plane direction ( $a_j$ ). The distance from a perforation in lamella *a* to the center of the next perforation in lamella *b* is  $d = \sqrt{c^2/4 + a^2/4}$ , resulting in  $d_a = 3.30$  nm,  $d_b = 3.18$  nm,  $d_c = 2.82$  nm,  $d_d = 2.54$  nm, and  $d_e = 2.72$  nm. The minimum and maximum values of the diameter of the perforations can be estimated by geometric considerations. For the maximum value of the perforation diameter a value somewhat smaller than half the lattice constant *a* can be assumed (i.e., ~2 nm). The minimum value for the diameter, ~1.3 nm, was found using an interdigitated arrangement of surfactant chains.

Within this structure, the perforations of complexes **3a** to **3c** are ordered *cI*, which can be seen in the scattering curve. But, because of the proposed underlying lamellar frame, the structure is not really cubic and therefore has to be called pseudocubic. A similar example to this is described by Antonietti et al.<sup>20</sup> who prepared a complex consisting of undulating rods that showed a SAXS pattern with cubic indexing. Furthermore, Maskos<sup>18</sup> investigated lamellar complexes for which a transition from a hexagonal to a disordered cubic type of undulations was found depending on the copolymer composition. For complexes **3d** and **3e**, showing the same perforated lamellar fundamental structure type as **3a** to **3c**, there is a clear difference in the in-plane direction and the direction perpendicular to the latter. It should be mentioned here that we can not exactly distinguish between perforated and undulated lamellar structures. This distinction has to be made by further experiment (e.g., by gas permeation measurements). A clear structure proof by scattering on the unoriented samples solely is impossible, and additional experimental evidence, such as electron microscopy or structure-sensitive solid-state NMR, is needed. These experiments are currently in progress.

Recently, Wang and Qi derived theoretically that there can be two different perforated lamellar structures for diblock copolymer melts. One structure is based on a *cI* lattice and one on an *hcp* lattice, with nearly degenerate free energy. This theory sufficiently explains the small-angle neutron scattering data for the *cI* type of perforations,<sup>21–23</sup> as well as that of *hcp* perforations in block copolymers.<sup>24</sup> Although this theory was derived for

(17) Hoffmann, H. *Ber. Bunsenges. Phys. Chem.* **1984**, *88*, 1078–1093.

(18) Antonietti, M.; Maskos, M. *Macromolecules* **1996**, *29*, 4199–4205.

(19) Kekicheff, P.; Tiddy, G. J. T. *J. Phys. Chem.* **1989**, *93*, 2520–2526.

(20) Antonietti, M.; Conrad, J. *Angew. Chem., Int. Ed. Eng.* **1994**, *33*, 1869.

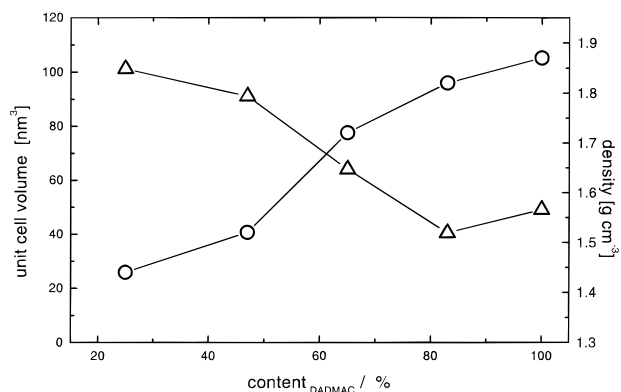


**Figure 5.** The unit cell volume (triangles) and the density (cycles) of the complexes depending on the content of diallyldimethylammonium. The diallyldimethylammonium content is given in mol % of the copolymer composition.

the microphase separation of block copolymers in the weak segregation regime, it seems to be reasonable to adopt some of their arguments to the PE-surfs described here. First, if we assume that there is an order parameter analogous to a dominant fluctuation that determines the lattice constant, we can then conclude that the wavelength of the fluctuation depends on the charge density. The higher the charge density, the shorter the fluctuation (i.e., a smaller lattice parameter). Furthermore, we found that a slight difference in the charge density from complexes **3c** to **3d** induces a phase transition from a *cI* to *tI* type perforations. This transition is indicative of nearly degenerate free energies of both types of perforations, which is similar to the situation found for block copolymers, for which a nearly degenerate free energy for *bcc* (*cI*) and *hcp* perforations was found.

Because there are two perforations in a unit cell of a *cI* as well as in a *tI* lattice, the unit-cell volumes can be compared directly. The unit-cell volume of all complexes as a function of the diallylmethylammonium content is presented in Figure 5 and listed in Table 3. It can be seen that with increasing cationic moieties, the unit cell volume shrinks from  $V_a = 101 \text{ nm}^3$ ,  $V_b = 91 \text{ nm}^3$ , and  $V_c = 64 \text{ nm}^3$  for the *cI* complexes to the lowest values of  $V_d = 40 \text{ nm}^3$  and  $V_e = 49 \text{ nm}^3$  for the *hcp* complexes. If the model of a perforated lamellar structure is correct, a shrinking volume per unit cell and a constant number of perforations in the lamellae increases their frustration (i.e., the deviation from a flat surface). So, we conclude that the higher the charge density of the polymer complex is, the higher is the curvature energy for the interface between the ionic polyelectrolyte-rich phase and the perfluoroalkyl-rich phase. The increasing curvature energy with increasing charge density is compensated by a higher Coulomb energy due to a denser packing of the ionic species. To verify this relationship we measured the bulk densities of the complexes. As expected, we found a considerable increase of the density with an increasing cationic monomer content. The lowest density of  $1.44 \text{ g/cm}^3$  was found for complex **3a** and the highest value of  $1.87 \text{ g/cm}^3$  was found for **3e** (see Figure 5 and Table 3).

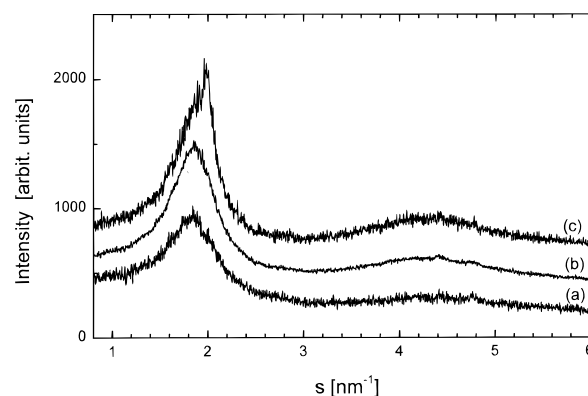


**Figure 6.** Wide-angle X-ray scattering diagrams of complexes **3a** to **3c**.

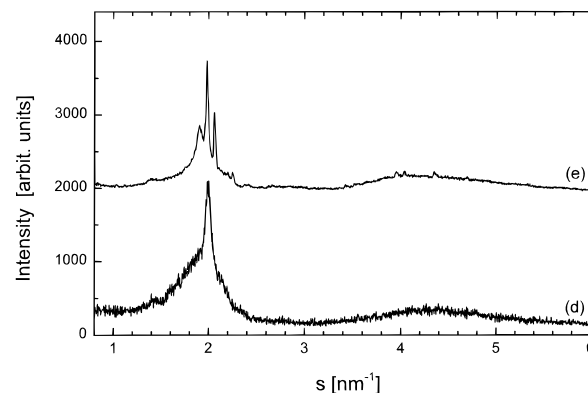


**Figure 7.** Wide-angle X-ray scattering diagrams of complexes **3d** and **3e**.

For the upper theoretical density limit, we expect a value somewhat lower than the density of amorphous poly(tetrafluoroethylene), which is  $\sim 2 \text{ g/cm}^3$ .<sup>25</sup> The data presented prove that the bulk density of the complexes can be varied strongly by variation of the charge density, and that the upper value reached approaches the theoretical limit.

**D. Wide-Angle X-ray Scattering.** From the strong increase in density found for the complex series, a change of order on an atomic lengthscale has to be expected. This expectation is confirmed by the WAXS data of the complex **3** films, which are presented in Figures 6 and 7. In the patterns of complexes **3a** to **3c**, only two broad maxima are found in the wide-angle region, indicating an amorphous fluoroalkyl chain packing. The position of their first maximum is similar and corresponds to *d*-values in the range of 0.52 to 0.55 nm. The peak width however, became significantly smaller from **3a** to **3c**, which is indicative of a denser packing in the same order, and therefore, is consistent with the observed increase in density. The similarity of the WAXS curves **3a** to **3c** supports the conclusion of isomorphic mesophases for **3a** to **3c** made earlier on the basis of SAXS data. In addition to two diffuse bands for complex **3d**, a narrow peak is found whose maximum position corresponds to  $d_d = 0.50 \text{ nm}$ . This peak is superimposed on a broad amorphous halo centered at a spacing of 0.53 nm. The most simple structure to explain the sharp WAXS-peak is a parallel alignment of rodlike perfluoroalkyl chains arranged in a 2D-hexagonal lattice with rotational disorder and an average distance of 0.57 nm between the rodlike chains. This value is close to that observed for a liquid crystalline

(21) Hamley, I. W.; Koppi, K. A.; Rosedale, J. H.; Bates, F. S.; Almdal, K.; Mortensen, K. *Macromolecules* **1993**, *26*, 5959–5970.

(22) Khandpur, A. K.; Förster, S.; Bates, F.; Hamley, I. W.; Ryan, A. J.; Bras, W.; Almdal, K.; Mortensen, K. *Macromolecules* **1995**, *28*, 8796–8806.

(23) Hajduk, D. A.; Harper, P. E.; Gruner, S. M.; Honeker, C. C.; Kim, G.; Thomas, E. L.; Fetters, L. J. *Macromolecules* **1994**, *27*, 4063–4075.

(24) Förster, S.; Khandpur, A. K.; Zhao, J.; Bates, F. S.; Hamley, I. W.; Ryan, A. J.; Bras, W. *Macromolecules* **1994**, *27*, 6922–6935.

(25) van Krevelen, D. W. *Properties of Polymers*; Elsevier: Amsterdam, 1990.

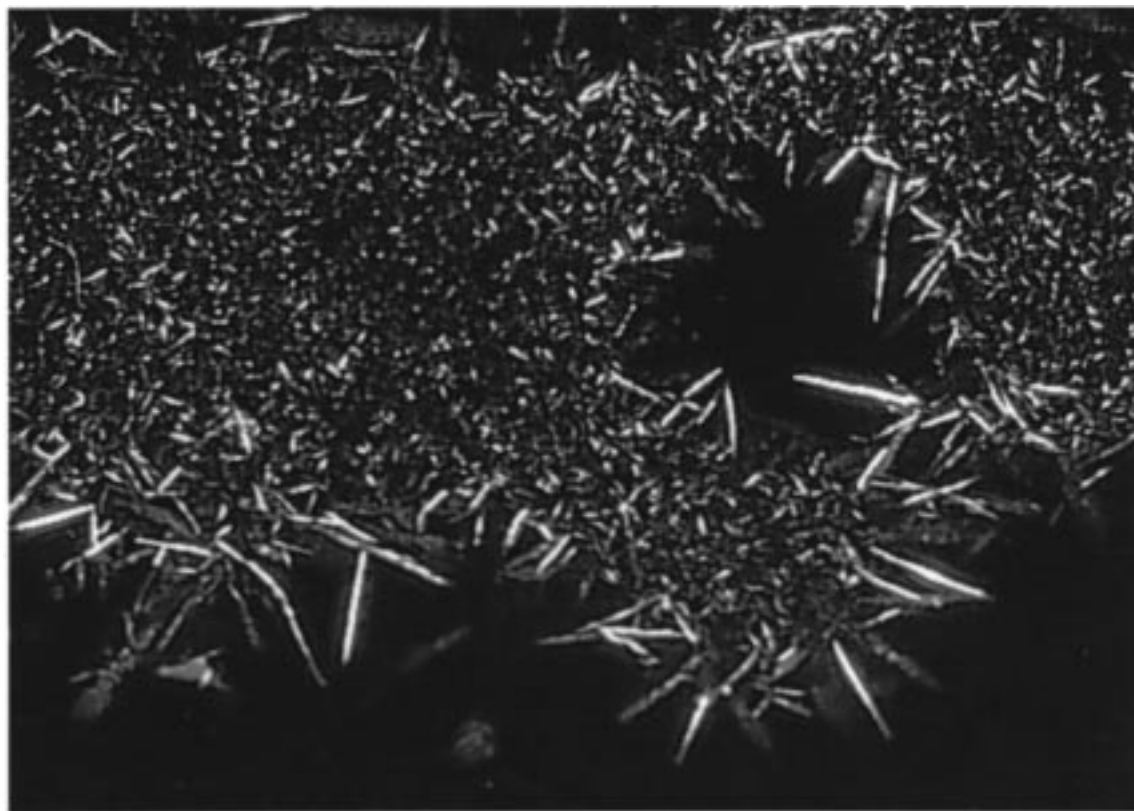


**Figure 8.** Optical micrograph of a complex **3e** film between crossed polarizers (magnification  $\times 20$ ).

phase of lithium octadecanoate (0.56 nm).<sup>19</sup> The qualitative difference in the WAXS curves of the complexes **3a** to **3c** compared with that of **3d** supports the interpretation of a transition in morphology from **3c** to **3d** made on the basis of SAXS data. In the WAXS curve of complex **3e**, three intense sharp maxima corresponding to  $d$ -values of 5.26, 5.05, and 4.85 nm, and several weak reflections are found. Because of the rigidity of the perfluoroalkyl chain, it is understandable to find a significant side-chain crystallinity for the relatively short  $C_{10}$ -carbon chain. In the case of polypeptide alkyl-surfactant complexes, a side-chain crystallinity is observed at first for an alkyl chain of 18 carbon atoms.<sup>1</sup> In contrast to complex **3d**, no rotational disorder exists for **3e**. The perfluoroalkyl chains of **3e** are organized on a well-defined crystal lattice.

**E. Optical Microscopy.** The films of the complexes **3a** to **3c** are completely transparent and optically isotropic. No birefringence was found during examination between crossed polarizers. This result is consistent with the SAXS data, from which isomorphous pseudocubic phases were determined for **3a** to **3c**. It is well known from cubic liquid crystals that they are non-birefringent, which often causes problems in identifying them.<sup>16</sup> In contrast to **3a** to **3c** a weak birefringence but no characteristic texture was found for complex **3d**. This result proves that **3d** does not show a cubic mesophase and therefore cannot be isomorphic to complexes **3a** to **3c**. The birefringence is in agreement with a tetragonal mesophase proposed on the basis of SAXS data. In contrast to the others, the crystalline complex **3e** shows a characteristic texture with needle-like crystals. The crystals have sizes up to 2 mm and a length-to-thickness ratio up to 16 to 1. An example of the optical textures is shown in Figure 8. Because of its appearance we call complex **3e** the blue needle-crystal phase. These needle-crystals are hybrids of polyelectrolytes and surfactants and differ from the pure surfactant crystals, which have different reflections

and melt at 83 to 85 °C. The strong birefringence is in agreement with a crystalline material with a supramolecular ordering of tetragonal symmetry as derived from SAXS data.

#### 4. Conclusions

Five solid complexes of poly[(diallyldimethylammonium chloride)-*co*-(*N*-methyl-*N*-vinylacetamide)] with perfluorodecanoate and 1:1 stoichiometry were prepared. The surface energies of the fluorinated complexes were in the range of 13 to 15 mN/m, which were independent of the fluorine content. This result was attributed to the formation of a surface of closely packed trifluoromethyl groups. From this result it can be suggested that the complexes are promising a new, nonstick coating materials. For all the complexes, stable self-organized mesophases were found. It is speculated that the building blocks of the mesophases are perforated lamellae. The perforations have a body-centered cubic or centered tetragonal order. With increasing charge density of the polymer, the number of perforations per unit volume and the bulk density increase strongly. From WAXS results it was derived that the packing order of the perfluoroalkyl chains increases with increasing charge density. However, only a complex with pure polydiallyldimethylammonium shows a significant side-chain crystallinity, whereas the others are amorphous on an atomic length scale.

**Acknowledgment.** The authors thank Dr. W. Jaeger for synthesis of the copolymers, C. Remde for help in preparation of the complexes, C. Burger for computational aid, M. Antonietti and C. Göltner for helpful discussion, and the Max-Planck Society for financial support.

LA971379E